CONF-730806--1

INTERCRYSTALLINE FRACTURE IN AN INTERNALLY OXIDIZED BCC ALLOY*

R. W. Carpenter and C. T. Liu
Metals and Ceramics Division
Oak Ridge National Laboratory
Oak Ridge, Tennessee 37830

Introduction

Intercrystalline fracture resulting from tensile deformation at low temperature, defined here as a temperature low enough that diffusion effects can be ignored, has been observed in several age-hardenable alloys having either a bcc or fcc matrix structure (1-6). These investigations have generally shown the alloys to have short elongation to fracture when aged to near maximum strength. The grain boundary facets on the fracture surface may be brightly reflective, and may be covered with a fine microdimple dispersion. These fractures are often termed brittle, although the existence of microdimples implies that localized shear fracture may have occurred. The relationship between fracture path, the precipitate free zone (PFZ), and the role of grain boundary precipitate is not clear, particularly in the case of the bcc alloys studied, because the grain boundary precipitate was thought to be the α-hcp form of either Hf or Ti, which is ductile at room temperature. The present work extends the fracture morphology study to a ductile bcc alloy precipitation hardened by oxide particles. We were particularly interested in the conditions under which microdimples could be observed on grain boundary fracture facets, and the size relationship between the microdimples and grain boundary precipitates.

Experimental Methods

A tantalum-base alloy containing nominally 8 w/o W and 2 w/o Hf was internally oxidized by annealing in a low pressure oxygen atmosphere at 1000°C for a time sufficient to gain 3000 ppm oxygen. This is a commercially produced alloy, known as T-111, and ordinarily used as a structural material for high temperature applications. Prior to oxidation treatment the specimens were recrystallized at 1500°C to produce an average grain size of 30 μ. Following the oxidation treatment some specimens were isothermally aged for various times at 1400°C, in vacuum, to cause precipitation of hafnium dioxide. Tensile specimens with microstructure corresponding to each different heat treatment, having a gage section size of 2.54 × 0.318 × 0.051 cm, were strained to fracture at room temperature using a constant cross-head speed of 0.127 cm/min.

*Research sponsored by the U.S. Atomic Energy Commission under contract with the Union Carbide Corporation.

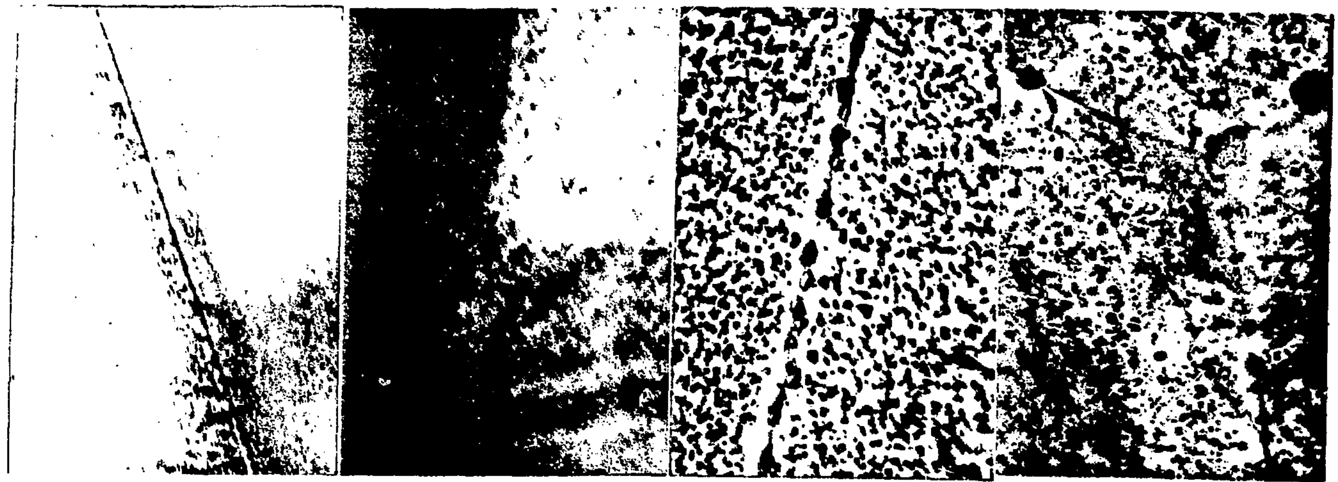

(a) (b) (c) (d)

FIG. 1

Microstructure of internally oxidized Ta-W-Hf alloy. TEM, 650 KV. (a) and (b) as oxidized; (c) aged 5 min; (d) aged 240 min. Magnification 104,400× for a,b,c. d:23,800×.

Observations

Internal Microstructure

An experimental investigation of the precipitation process accompanying internal oxidation of this alloy at 1000°C followed by isothermal aging at higher temperatures established that the precipitate is HfO_2; a study of the precipitation process will be published elsewhere. Examples of the microstructures observed are shown in Fig. 1. After oxidation at 1000°C, called the "as-oxidized" condition, a homogeneous dispersion of Hf-O zones exists in the matrix (Fig. 1a and 1b). It can be seen in Fig. 1a that the grain boundary regions, viewed edge on, consisted of a dark continuous band about 50 Å thick on the boundary itself, a thin more or less continuous white band on each side of the boundary, and a thicker band of relatively dark contrast on the outside of each white band. The inner white band and outer dark band are about 50 Å and 400 Å thick, respectively. In Fig. 1b, where grain boundaries are observed obliquely, it is seen that there is in fact no continuous precipitate layer in the boundary, but rather a high density of very small precipitate particles. The thin white band on either side of the grain boundary are believed to be regions of zone depletion, i.e., precursors of the fully developed PFZ regions in the aged alloys. It has been suggested that they may be an electropolishing artifact (7). Such grain boundary sensitivity to electropolishing is a well known effect in precipitation systems, and may be a contributing factor. It is probably not the major cause in this case, since well developed PFZ occurred in aged specimens and selective thinning at grain boundaries was not a major effect (see Fig. 1c,1d). The wider dark bands on each side of the grain boundary in Fig. 1a are also due to inhomogeneous solute distribution, since they were not observed in recrystallized or aged specimens. Microhardness traverses (data not shown) show a linear decrease in hardness from surface to center line for as-oxidized specimens. The center line hardness is about 17% lower than the surface, independent of average oxygen concentration over a broad range, and at 3000 ppm the center line hardness is 3.2 times greater than the recrystallized alloy. No difference in zone structure was noted in specimens taken from near the surface or on the center line. The hardness gradient rapidly disappears in aged specimens, indicating that the small initial oxygen gradient is flattened by aging. Upon aging at 1400°C, incoherently diffracting HfO_2 precipitate formed and coarsened rapidly. Well defined PFZ and grain boundary precipitate formed (Fig. 1c,1d). As aging time lengthened, PFZ width increased and the relative size of precipitate type, at any stage of aging, was matrix, grain boundary, and triple point, in ascending order. It can be seen from Fig. 1d, that on some grain boundaries precipitates were more closely spaced and smaller than on others. This is a boundary misorientation effect and has been observed in other alloys (8). Since the grain size of the specimens was much smaller than the minimum cross-sectional dimension of the gage section a simple average of precipitate size and PFZ width was used to characterize a particular microstructure. We note that all aged specimens examined had well-defined PFZ and grain boundary precipitate on all observed boundaries.

Mechanical Properties

The engineering stress-strain behavior of the alloy in the recrystallized, as oxidized, and several aged conditions is shown in Fig. 2. The aged specimens exhibited a decreasing initial yield stress and increasing strain to fracture as aging time increased. All the aged specimens underwent general yielding before fracture. The generally higher slope of the plastic region of the curves for aged specimens relative to the recrystallized condition infers that precipitates were not sheared by mobile dislocations after aging times longer than a few minutes. The as-oxidized specimen fractured at an anomalously low stress, before general yielding occurred. Microhardness measurements showed the as-oxidized state to be harder than any other, and the fracture mode of this specimen was complicated by the presence of transgranular cleavage, as shown below.

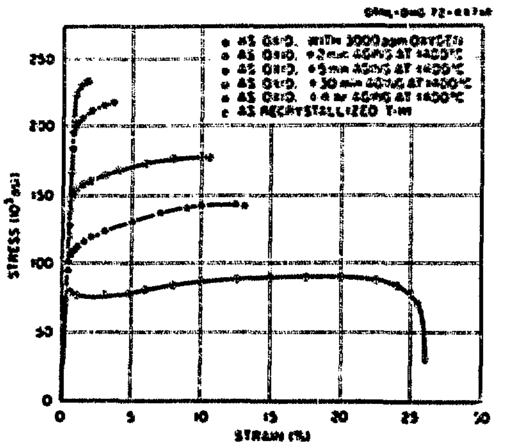

FIG. 2
Engineering Stress-Strain Curves.

Fracture Morphology

The basic fracture mode of the recrystallized alloy was ductile shear. A typical example is shown in Fig. 3, a view of the fracture surface with the width dimension arranged horizontally. The "cup" portion of the fracture is seen running across the figure; many coalesced microdimples are visible on its bottom portion. The cup is bounded by two prominent shear lips. The upper part of Fig. 3 shows some external specimen surface on which can be seen coarse wavy slip bands, and large accomodation strains at grain boundaries. No cracks at grain boundaries or triple points were observed on this specimen. Specimens containing oxygen underwent a complete change in fracture morphology. The fracture surfaces of as-oxidized and 2 min aged specimens exhibited regions of transgranular cleavage and grain boundary separation. A typical example of the mixed mode for the as-oxidized specimen is shown in Fig. 4a. Specimens aged longer than 2 min fractured entirely by grain boundary separation, shown in Fig. 5. It can be clearly seen that the grain boundary facets on aged specimens are covered with microdimples. Further, the microdimple size increases with aging time. The average microdimple size, determined from SEM photographs, is plotted along with average grain boundary ppt and PFZ size in Fig. 6. All three parameters increase in a very similar way with aging time. It was noted earlier that triple point precipitates were consistently larger than grain boundary precipitates; the grain edge microdimples seen in Fig. 5 on the specimens aged 30 min and 4 hr correspond to triple points seen in TEM, and they are larger than the corresponding facet face microdimples. These observations lead naturally to the conclusion that grain boundary and triple point precipitates acted as microvoid nuclei, and that many of the microdimples on grain boundary fracture facets should have precipitate particles in them. This was easily observed to be true in specimens aged for longer times, but became more difficult for those aged 2 min or 5 min, probably because the precipitate is quite small at shorter times. The direct correlation between microdimple size and grain boundary precipitate and PFZ size leads one to expect observation of even smaller microdimples on grain

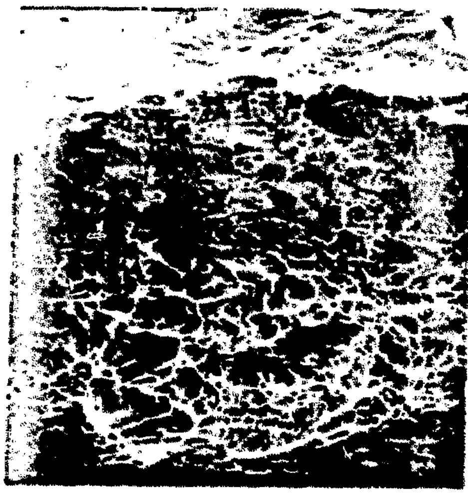

FIG. 3
Recrystallized alloy fracture, 500×

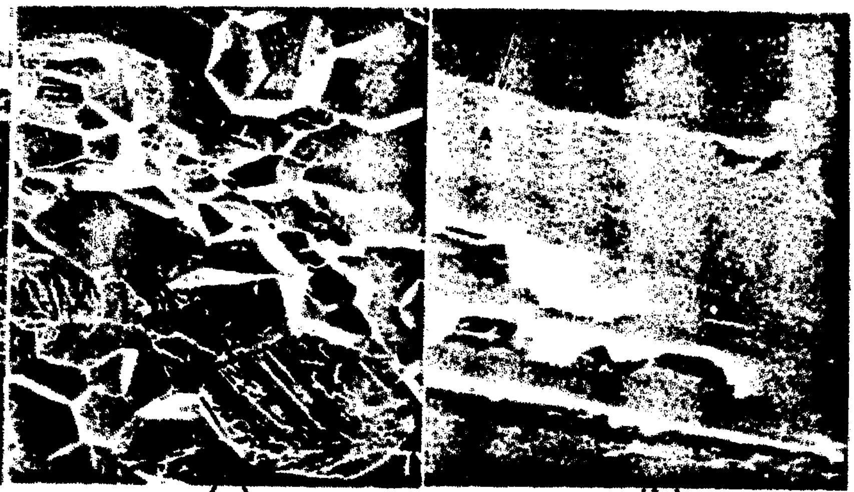

(a) (b)

FIG. 4
As-oxidized alloy fracture. (a) 500×, (b) 10,000×.

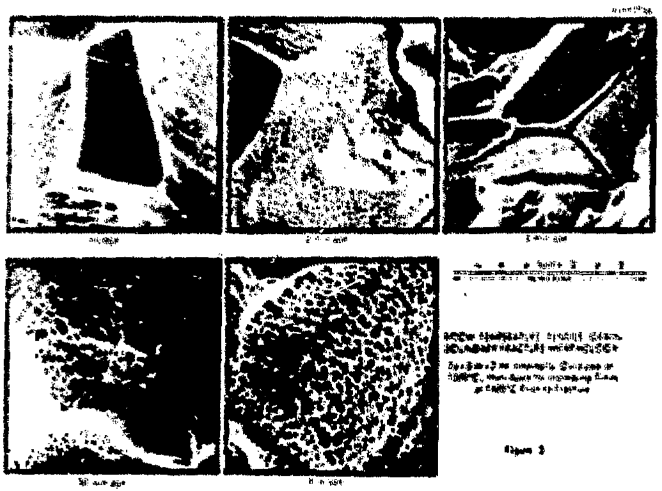

FIG. 5

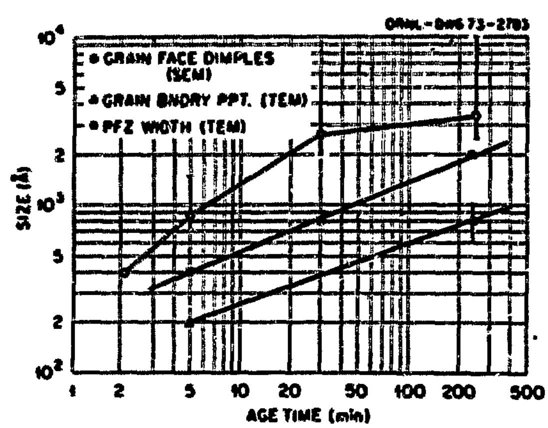

FIG. 6

boundary fracture facets of the as-oxidized specimens. These proved difficult to detect by SEM techniques. Region A of Fig. 4b shows an example of the surface modulations observed on grain boundary fracture facets of the as-oxidized specimen. The facets are generally quite flat, and the contrast modulations interpreted as evidence of the existence of very small microdimples is quite dependent on specimen tilt, which indicates the observation is real and not an electronic artifact. The bright shear lips extending away from the lower part of the facet shown in Fig. 4b are further evidence of localized plastic strain in the grain boundary regions of this specimen. Although a diligent search was made, no evidence of "cleavage" on grain boundary fracture facets was observed in any case, either on the aged or as-oxidized specimens. The transgranular cleavage observed on the as-oxidized and 2 min aged specimens can be seen (Fig. 4a) to have occurred only in isolated grains and thus is related to the orientation of individual grains relative to the stress axis. The geometric arrangement of the river patterns indicates that the cleavage cracks originated at grain boundaries. The most probable nucleation mechanism is the intersection of one of the rather widely spaced intense slip bands visible as bright lines on facets of the as-oxidized specimen (Figs. 4a and 5) with a grain oriented to favor cleavage.

Discussion

The experimental findings presented show that whenever grain boundary separation, or alternatively intercrystalline fracture, was observed in this alloy it could best be described as localized ductile fracture. Because of the relatively small strain to fracture observed for the oxygen containing alloy and the low magnification appearance of the intercrystalline fractures this alloy could be described as brittle on a macroscale. However, the microscopic intercrystalline fracture process is clearly microvoid growth and coalescence in the grain boundary regions; these regions are defined to be the grain boundary and its associated PFZ volume. The decreasing scale of the microdimple dispersion is a direct result of the small size of the grain boundary precipitate and PFZ at shorter aging times; experimental verification of localized ductile fracture will become increasingly more difficult at shorter aging times for all alloys of this type. When the present results are compared to earlier work on bcc alloys with ductile grain boundary precipitates (1), one finds the same microdimpled grain boundary fracture facet morphology. This fracture process involving localized microvoid growth and coalescence is at least qualitatively independent of the mechanical properties of the precipitate, and apparently only depends on the existence of a PFZ weaker to some extent than the surrounding matrix. This is consistent with simple theoretical models treating the apparent strengthening of a weak layer of metal constrained between and geometrically restrained during plastic deformation by stronger metal (9). Under these conditions microvoids can grow and coalesce under the influence of induced hydrostatic tension or intense local shear in the weak layer (10).

References

1. R. W. Carpenter, p. 667; R. J. Livak and W. W. Gerberich, p. 647; G. H. Narayanan and T. F. Archbold, p. 657 in "Electron Microscopy and Structure of Materials," Ed. by G. Thomas, R. M. Fulrath and R. M. Fisher, University of California Press (1972).

2. P.N.T. Unwin and G. C. Smith, J. Inst. Metals 97, 299 (1969).

3. D. E. Porter, UCRL-19004; Thesis (1969) University of California.

4. D. A. Ryder and A. G. Smale, p. 237 in "Fracture of Solids," 20, Met. Soc. Conf., AIME-IMD, ed. by D. C. Drucker and J. J. Gilman, Gordon and Breach (1963).

5. G. Thomas and J. Nutting, J. Inst. Metals 88, 81 (1959/60).

6. A. H. Geisler, Trans. AIME 180, 230 (1949).

7. K. Farrell, personal communication.

8. P.N.T. Unwin and R. B. Nicholson, "Nucleation and Initial Stages of Growth of Grain Boundary Precipitates in Al-Zn-Mg and Al-Mg Alloys" (preprint).

9. E. Orowan, J. F. Nye, and W. J. Cairns; Rept. No. 8, p. 173, "Strength and Testing of Materials," Part I, 6, London, H. M. Stationery Office (1952).

10. A. J. West, H. J. Saxton, A. S. Tetelman and C. R. Barrett, Met. Trans. 2, 1009 (1971).